A PERFECT-CROSS-FLOW MODEL FOR TWO PHASE FLOW IN POROUS MEDIA

by
Douglas Ruth and Jonathan Bartley
University of Manitoba

ABSTRACT

The present paper will report results for a "perfect-cross-flow" model. This is essentially a one-dimensional parallel tube model. However, it is assumed that fluid can flow without resistance between any tubes that contain the same phase (oil or water) at a given location. By comparing results from this model with results from a conventional two-phase numerical simulator (based on the modified Darcy law), it is shown that the perfect-cross-flow model is an exact analogy to the modified Darcy law. Using the model, it is shown that the commonly assumed boundary condition of gradually increasing capillary pressure at the inlet and outlet faces of a sample is inconsistent with the microscopic behavior of the porous media. This can lead to significant errors in data interpretation. It will also be argued that because real porous media do not demonstrate perfect-cross-flow, it is possible that two-phase displacement flows cannot always be modeled using the modified Darcy law.

INTRODUCTION

A major impediment to quality control in core analysis is a lack of standard samples with which to validate data. The petrophysical properties (porosity, permeability, capillary pressure, relative permeability, etc.) of both natural and synthetic "standard" samples are not known *a priori*. Furthermore, these properties can vary with time and use. Therefore, the best that we can do is compare one data set to another; that is, we can determine precision but not accuracy. For some properties, this criticism can be extended to data analysis techniques. Whereas data reduction methods for such properties as porosity and permeability are direct, hence introduce no additional errors, methods for properties such as capillary pressure and relative permeability involve inverse methods that can introduce errors. For capillary pressure, idealized models can be used to generate model data sets that can then be used to validate data reduction techniques. However, the idealized models for unsteady state relative permeability experiments do not generally conform to real data sets.

In the past, researchers have attempted to model two-phase flow in porous media in many ingenious ways. For example, Purcell [1] modeled the capillary pressure and saturation relationship using a bundle of parallel tubes; Yuster [2] analytically considered the simultaneous annular flow of oil and water through a single capillary tube and also in a series of connected tubes, each of a different diameter. Others have modeled relative permeability and trapping of oil in irregularly shaped conduits (e.g., Danis and Jacquin [3]). Large-scale network modeling of porous media has been done using lattice networks of pores and throats, in a range of connection patterns, varying from straight tubes to

sinusoidal-shaped tubes, and nodes of zero volume to nodes of spherical volume (e.g., Lin and Slattery [4]; Payatakes and Dias [5]; Koplik and Lasseter [6]). Recent efforts in network modeling have also included developing three-dimensional networks (e.g., Constantinides and Payatakes [7], Blunt and King [8]). Common numerical methods for network modeling include rule-based algorithms that model the invasion and displacement of fluids using pore-size and throat-size distribution functions (with possible spatial correlation) that define the pore-scale geometry and determine local fluid viscous resistances and local pressure discontinuities (e.g., Blunt [9]). Another approach is the dynamic network modeling method, where the interfaces between phases are tracked over time as they progress through the pore spaces, yielding detailed information about local flow rates and pressures of each phase (e.g. Dias and Payatakes [10], Constantinides and Payatakes [7], Mogensen and Stenby [11], Dahle and Celia [12]).

There are two fundamental approaches to studying two-phase flow in porous media. One is to attempt to model the actual flow paths in naturally occurring flows such as those through sand or rock. The second is to treat a network model as being a theoretical form of porous media and interpret the results as pseudo-experimental data (*e.g*., Bartley and Ruth [13,14]). The advantage of the second approach is that one can apply mathematical theories that seek to describe the flow in any porous medium (such as the modified Darcy law for two-phase flow (MDL)) to the special case of the network model flow, and compare predicted quantities with directly calculated quantities. A network model that lends itself to this type of modeling is the bundle of capillary tubes or parallel tube model (PTM). In this case, one is able to accurately track the oil/water interfaces as they progress through the tubes and also to calculate the pressures at any point in the model. Closed-form equations for flow in a bundle of tubes can be developed. The model is rigorous and limited only by the assumptions of steady, fully developed laminar flow. The obvious limitation to the PTM is that no cross-flow occurs between the tubes, and some would argue that this disqualifies the model from being considered a porous medium; however, the PTM does fall within the general definition of a porous medium. Consider now the opposite scenario where we are still analyzing flow in a bundle of tubes, but fluids are allowed to cross over from tube-to-tube at any location along the length of the tube bundle, provided only that both tubes contain the same fluid. That is, we are attempting to describe a scenario where the resistance to flow between the tubes is zero (perfect-cross-flow occurs) and there is no pressure difference between the same fluid in different tubes at the same location (perfect pressure equalization between the tubes). Furthermore, there are no capillary effects between tubes. This model is another theoretical construction that qualifies as a porous medium. Implementation of the model involves tracking two fluid components (water and oil) that occupy varying portions of separate capillary tubes. Within each tube there is hydraulic resistance to flow and a capillary interface. The calculation of this type of flow (injection of a wetting phase) models immiscible displacement of the non-wetting phase from the tube bundle.

The assumptions behind the perfect-cross-flow model (PCFM) were first proposed by Dong *et al* [15]. These assumptions are counter-intuitive. If flow paths exist between

tubes, the flow paths must offer resistance. Furthermore, these flow paths should allow water to invade an oil-filled tube from a water-filled tube. However, both tube-to-tube flow resistance and tube-to-tube fluid invasion are explicitly excluded in the PCFM.

MODEL FORMULATION

The essential features of the PCFM can be demonstrated by considering the set of three parallel tubes shown in Figure 1. The interfaces within the tubes subdivide the problem into four regions. It will be assumed that the flow of a single phase in any tube is governed by the Hagen-Poiseuille expression

$$Q_\alpha = \frac{\pi \delta^4}{128 \mu_\alpha} \frac{dP_\alpha}{dx} \quad (1)$$

where the α denotes the phase. The flow in each region is governed by the following expressions, which are obtained by summing the flows in the tubes in the region, separately by phase (the nomenclature is given in Figure 1):

$$Q_{w1} = \frac{\pi (P_{wi} - P_{w1})}{128 \mu_w L_1} \left(\delta_1^4 + \delta_2^4 + \delta_3^4\right) \quad (2a)$$

$$Q_{w2} = \frac{\pi (P_{w1} - P_{w2})}{128 \mu_w (L_2 - L_1)} \left(\delta_2^4 + \delta_3^4\right) \qquad Q_{o2} = \frac{\pi (P_{o1} - P_{o2})}{128 \mu_o (L_2 - L_1)} \delta_1^4 \quad (2b)$$

$$Q_{w3} = \frac{\pi (P_{w2} - P_{w3})}{128 \mu_w (L_3 - L_2)} \delta_3^4 \qquad Q_{o3} = \frac{\pi (P_{o2} - P_{o3})}{128 \mu_o (L_3 - L_2)} \left(\delta_1^4 + \delta_2^4\right) \quad (2c)$$

$$Q_{o4} = \frac{\pi (P_{o3} - P_{oe})}{128 \mu_o (L - L_3)} \left(\delta_1^4 + \delta_2^4 + \delta_3^4\right) \quad (2d)$$

Furthermore, by the definition of capillary pressure, for any tube j

$$P_{cj} = P_{oj} - P_{wj} \quad (3)$$

where

$$P_{cj} = \frac{4 \sigma \cos\theta}{\delta_j} \quad (4)$$

By continuity, for any region j

$$Q_t = Q_{wj} + Q_{oj} \quad (5)$$

where Q_t is the total flow. Equations 1 through 5 may be combined to yield the expressions

$$Q_t \frac{L_1}{\lambda_{w1} + \lambda_{w2} + \lambda_{w3}} = P_{wi} - P_{w1} \quad (6a)$$

$$Q_t \frac{L_2 - L_1}{\lambda_{o1} + \lambda_{w2} + \lambda_{w3}} - \frac{\lambda_{o1}}{\lambda_{o1} + \lambda_{w2} + \lambda_{w3}} (P_{c1} - P_{c2}) = P_{w1} - P_{w2} \quad (6b)$$

$$Q_t \frac{L_3 - L_2}{\lambda_{o1} + \lambda_{o2} + \lambda_{w3}} - \frac{\lambda_{o1} + \lambda_{o2}}{\lambda_{o1} + \lambda_{o2} + \lambda_{w3}} \left(P_{c2} - P_{c3}\right) = P_{w2} - P_{w3} \quad 6c$$

$$Q_t \frac{L - L_3}{\lambda_{o1} + \lambda_{o2} + \lambda_{o3}} - \left(P_{c3} - P_{oe}\right) = P_{w3} \quad 6d$$

where

$$\lambda_{\alpha j} = \frac{\pi}{128\,\mu_\alpha} \delta_j^4 \quad 7$$

This set of four equations contains nine unknowns: Q_t , P_{wi}, P_{w1}, P_{w2}, P_{w3}, P_{oe}, L_1, L_2, and L_3. The system of equations will allow for two boundary conditions. These will typically be Q_t or P_{wi}, and P_{oe}, all possibly as functions of time. Given two of these quantities, the third can be obtained by summing the governing equations to yield

$$Q_t \left[\frac{L_1}{\lambda_{w1} + \lambda_{w2} + \lambda_{w3}} + \frac{L_2 - L_1}{\lambda_{o1} + \lambda_{w2} + \lambda_{w3}} + \frac{L_3 - L_2}{\lambda_{o1} + \lambda_{o2} + \lambda_{w3}} + \frac{L - L_3}{\lambda_{o1} + \lambda_{o2} + \lambda_{o3}} \right] - \frac{\lambda_{o1}}{\lambda_{o1} + \lambda_{w2} + \lambda_{w3}} \left(P_{c1} - P_{c2}\right) - \frac{\lambda_{o1} + \lambda_{o2}}{\lambda_{o1} + \lambda_{o2} + \lambda_{w3}} \left(P_{c2} - P_{c3}\right) - P_{c3} = P_{wi} - P_{oe} \quad 8$$

Therefore, if the lengths are known, all other parameters can be calculated.

Given initial conditions for the lengths, typically all lengths equal to zero, the complete solution requires solving the following set of differential equations:

$$\frac{dL_1}{dt} = \frac{4\left(Q_{w1} - Q_{w2}\right)}{\pi\,\delta_1^2} \qquad \frac{dL_2}{dt} = \frac{4\left(Q_{w2} - Q_{w3}\right)}{\pi\,\delta_2^2} \qquad \frac{dL_3}{dt} = \frac{4\,Q_{w3}}{\pi\,\delta_3^2} \quad 9$$

Combining the governing equations and using the continuity equations we can derive explicit expressions for the flow of water

$$Q_{w1} = Q_t \quad 10a$$

$$Q_{w2} = Q_t \frac{\lambda_{w2} + \lambda_{w3}}{\lambda_{o1} + \lambda_{w2} + \lambda_{w3}} + \frac{P_{c2} - P_{c1}}{L_2 - L_1} \lambda_{o1} \frac{\lambda_{w2} + \lambda_{w3}}{\lambda_{o1} + \lambda_{w2} + \lambda_{w3}} \quad 10b$$

$$Q_{w3} = Q_t \frac{\lambda_{w3}}{\lambda_{o1} + \lambda_{o2} + \lambda_{w3}} + \frac{P_{c3} - P_{c2}}{L_3 - L_2} \lambda_{w3} \frac{\lambda_{o1} + \lambda_{o2}}{\lambda_{o1} + \lambda_{o2} + \lambda_{w2}} \quad 10c$$

$$Q_{w4} = 0 \quad 10d$$

For the present paper, these equations were solved using a fully implicit, iterative scheme. The size of a time step was calculated as the interval required for the fluid in the most advanced interface to move a given distance Δx. For example, in the 3-tube model, in the time period before Tube #3 reaches the exit face, this time interval is given by the expression

$$\Delta t = \frac{\Delta x \, \pi \, \delta_3^2}{4 \, Q_{w3}} \qquad 11$$

Given this time step, the values for the new lengths of displacement in all of the tubes were found by iterating on the equations until a sufficiently converged solution was obtained.

MODEL OPERATION

To start the model, the interface in Tube #3 is advanced by the increment Δx. Initially L_1 and L_2 are set to zero. Only the equations for motion in Regions #3 and #4 are required (the equations for Region #1 and Region #2 are not required because of the zero lengths of these regions). In Region #2 oil is initially assumed to be immobile and the pressure at L_3 is determined. The condition for flow to initiate in Tube #2 is that

$$P_{wi} + P_{c2} > P_{w3} + P_{c3} \qquad 12$$

If this condition obtains, then L_2 is set to a small value ($L_2 < L_3$) and iterations are performed until a converged solution has been obtained. Note that this iteration now includes the equations for Region #2 but it is still assumed that oil is immobile in Region #1. A test is then made for flow in Tube #1. Once all of the interfaces that are going to start have been identified and values for flows and pressures have been obtained by an iterative scheme, the solution for that time step is complete. At each further time step, tests are done to ensure that any new interfaces can start if the proper conditions obtain.

The upstream boundary condition is usually specified either as $Q_t(t)$ or as $P_{wi}(t)$. Often the functions are constants; in fact, most laboratory experiments are designed for either constant flow or constant injection pressure. However, even if these functions are constants, complications can arise. Consider the case of constant flow rate at such a value that only Tube #3 starts during early time steps. If the condition for Tube #2 to start is not met, then conditions are actually appropriate for oil to flow backwards in Region #3 and be produced from the injection face of the sample. Most apparatuses prevent this from happening by proper design of the injection manifold. However, for some designs, such as an upstream plenum, production of oil at the injection face can occur.

If it is assumed that oil can be produced from the injection face of the sample, and such production is to be accurately calculated, then the appropriate pressure condition for the oil at the inlet must be identified. The "obvious" choice is to allow the saturation at the inlet to dictate the capillary pressure difference between the oil and the water. In the case where only Tube #3 has started, this is equivalent to letting P_{c2} determine the pressure of the oil at the inlet; hence, the pressure difference across the oil in Region #3 would be $P_{wi} + P_{c2} - P_{w3} - P_{c3}$. However, this is not consistent with the perfect-cross-flow assumption. For perfect cross-flow, the oil will be produced from the tube offering the least capillary resistance, that is, from Tube #1. Hence, to be consistent with the PCFM, the actual pressure difference across the oil in Region #3 is $P_{wi} + P_{c1} - P_{w3} - P_{c3}$. In the simulations performed for the present paper, production of oil at the inlet was suppressed.

The downstream boundary condition also needs special consideration. First, the fluid that contacts the exit face must be specified. Depending on experimental design, water may contact the exit face (a water filled plenum design), oil may contact the exit face (a design where oil is flushing the produced fluids at the exit face), or both oil and water may contact the exit face (a well-designed manifold). If both oil and water contact the exit face, then it can be assumed that both P_{we} and P_{oe} are zero (no capillary pressure can exist outside of the sample). If water contacts the exit face, then imbibition of water (assuming water-wet conditions) is possible, with water entering Tube #3 (the tube with the highest capillary pressure). Simultaneous with this mechanism, oil will be produced due to the imposed overall flow rate. Using a "path of least capillary resistance" argument similar to that given above, the pressure seen by the oil at the exit face will be P_{c1}.

If oil contacts the exit face, then the potential for capillary trapping exists. Even if all of the oil in Tube #3 has been displaced by water, the water cannot exit the sample until the pressure of the water at the upstream end of Region #3 (Region #4 no longer exists) is greater than P_{c3}. It follows that the boundary condition on the water is either

$$P_{we} = P_{w2} \qquad for \qquad P_{w2} < P_{c3} \tag{13a}$$

$$P_{we} = P_{c3} \qquad for \qquad P_{w2} > P_{c3} \tag{13b}$$

PROPERTIES OF A COREY MEDIUM

In the present paper, the PCFM will be applied to a "Corey" medium. A Corey medium is defined as a porous media that has parallel tube-like flow channels that have a diameter distribution density, ρ, defined by the expression

$$\frac{d\rho}{d\delta} = \delta^{\lambda} \tag{14}$$

The following equations for properties may then be derived from basic equations:

Porosity (ϕ)

$$\phi = \frac{\pi}{4\,A} \int_0^{\delta_m} \delta^2 \, d\rho = \frac{\pi}{4\,A} \int_0^{\delta_m} \delta^{2+\lambda} \, d\delta = \frac{\pi}{4\,A\,(3+\lambda)} \, \delta_m{}^{3+\lambda} \tag{15}$$

Permeability (k)

$$k = \frac{\pi}{4\,A} \int_0^{\delta_m} \delta^4 \, d\rho = \frac{\pi}{4\,A} \int_0^{\delta_m} \delta^{4+\lambda} \, d\delta = \frac{\pi}{4\,A\,(5+\lambda)} \, \delta_m{}^{5+\lambda} \tag{16}$$

Saturation of water (S_w)

$$S_w = \frac{\int_0^{\delta} \delta^2 \, d\rho}{\int_0^{\delta_m} \delta^2 \, d\rho} = \frac{\int_0^{\delta} \delta^{2+\lambda} \, d\delta}{\int_0^{\delta_m} \delta^{2+\lambda} \, d\delta} = \left(\frac{\delta^{2+\lambda}}{\delta_m{}^{2+\lambda}} \right)^{3+\lambda} \tag{17}$$

Capillary pressure (P_c)

$$\frac{P_c}{P_{ct}} = \frac{\delta_m}{\delta} = \frac{P_{ct}}{S_w^{1/(3+\lambda)}} \qquad 18$$

Relative permeability (k_{rw})

$$k_{rw} = \frac{\int_0^{\delta} \delta^4 \, d\rho}{\int_0^{\delta_m} \delta^4 \, d\rho} = \frac{\int_0^{\delta} \delta^{4+\lambda} \, d\delta}{\int_0^{\delta_m} \delta^{4+\lambda} \, d\delta} = \frac{\delta^{5+\lambda}}{\delta_m{}^{5+\lambda}} = S_w^{(5+\lambda)/(3+\lambda)} \qquad 19$$

Relative permeability (k_{rnw})

$$k_{rnw} = 1 - S_w^{(5+\lambda)/(3+\lambda)} \qquad 20$$

Figure 2 shows relative permeability and capillary pressure curves for $\lambda=3$, the value used for the simulations reported in the present paper. The relative permeabilities sum to 1.0 because all of the fluid is mobile in the PCFM.

SOME PRELIMINARY RESULTS

Solutions were obtained for a PCFM model with 60 capillary tubes having a size distribution consistent with the curves in Figure 2. It was assumed that water contacted the exit face. Figure 3 shows saturation profiles for a range of viscosity ratios and two volumetric flow rates. The volumetric flow rates are normalized with the flow rate that would result for water with a pressure differential equal to the maximum capillary pressure (smallest capillary tube). The viscosity ratio is the viscosity of the oil divided by the viscosity of water. All of the curves in Figure 3 represent a point in the displacement process where 20% of the original oil in place has been produced. The wide variation in behavior is evidence of the importance of viscosity ratio and flow rate to the displacement process.

Figures 4 and 5 show comparisons between results obtained by using the perfect cross-flow model and results obtained by using a conventional numerical simulator based on the MDL. In order to allow direct comparisons with the MDL, the exit boundary condition for these simulations was based on the exit saturation. The input parameters to this model were the relative permeability and capillary pressure curves calculated for the PCFM, plus the petrophysical properties for that model. The results are calculated directly, without any adjustments, that is, the results were not history-matched. The water and oil production curves appear to give an exact agreement; this is partly attributed to the scale; small discrepancies can be seen in the actual data. The results for pressure again show excellent agreement. The saturation profiles for the PCFM are plotted as a series of steps; a stepped profile more accurately reflects the nature of the saturation changes at the fronts in each tube. The saturation profiles show small disagreements, with the simulation results being slightly below the PCFM results; this may be due to numerical dispersion. In general the agreement is very good.

THE INFLUENCE OF THE EXIT BOUNDARY CONDITION

The PCFM was applied to demonstrate the influence of using different capillary pressure criteria at the exit face. As noted above, this capillary pressure is usually calculated based on the saturation at the exit face. To be consistent with the PCFM, the exit capillary pressure should correspond to the capillary pressure in the largest tube, that with the lowest capillary pressure. Figure 6 shows a comparison of the differential pressure as a function of time for the two boundary conditions. Clearly the two data sets would not lead to the same results if analyzed to determine relative permeabilities.

THE VALIDITY OF THE MODIFIED DARCY LAW

The PCFM casts doubt on the validity of the MDL as it is applied to multi-phase flow. Bartley and Ruth [13,14] have shown that the MDL gives results that are inconsistent with results calculated with the PTM. Specifically, the PTM leads to relative permeability curves that are functions of both saturation and position. It has been demonstrated in the present paper that the PCFM is consistent with the MDL. The problem is that real porous media cannot conform completely with the PCFM because perfect cross flow is a physically impossible situation (although we suggest that flow in unconsolidated sands may approach the model). It seems reasonable that flow in real porous media would fall somewhere in between the two cases of the PCFM and the PTM. The following logic would therefore apply: the PCFM yields results that are consistent with the MDL; the PTM yields results that are inconsistent with the MDL; the PTM and the PCFM bound the behavior of real porous media; therefore, the MDL is not necessarily valid for real porous media.

CONCLUSIONS

The results described in the present paper support the following conclusions:

1. For the limited test cases investigated, the PCFM yields results that are consistent with the MDL.
2. The boundary conditions generally imposed on two-phase displacement experiments are inconsistent with the PCFM.
3. Preliminary results suggest that the MDL may not be applicable to all porous media.

Acknowledgments: This work was supported by an NSERC operating grant. One of the authors (JB) was supported by an NSERC graduate scholarship.

REFERENCES

1. Purcell, W.R., "Capillary Pressures -Their Measurement Using Mercury and The Calculation of Permeability Therefrom," *Trans. AIME*, (1949) **186**, 39–48.
2. Yuster, S.T., "Theoretical Considerations of Multiphase Flow in Idealized Capillary Systems," in: *Proc. of the 3rd World Petroleum Congress*, Section II, (1951) The Hague, pp.437–445.
3. Danis, M. and Ch. Jacquin, "Influence du Contraste de Viscosités sur les Perméabilités Relatives lors du Drainage Expérimentation et Modélisation," *Revue de l'Institut Français du Pétrole*, (1983) **38**, 6, 723–733.
4. Lin, C.Y. and J.C. Slattery, "Three-Dimensional, Randomized, Network Model for Two-Phase Flow through Porous Media," *AIChE J.*, (1982) **28**, 2, 311–324.
5. Payatakes, A.C. and M.M. Dias, "Immiscible Microdisplacement and Ganglion Dynamics in Porous Media," in: Amundson, N.R. and D. Luss (eds.) *Reviews in Chemical Engineering*, (1984) **2**, 2, D. Reidel Publishing Co., Dordrecht, and Freund Publishing House Ltd., London, pp.85–174.
6. Koplik, J. and T.J. Lasseter, "Two-Phase Flow in Random Network Models of Porous Media," *Soc. Petrol. Eng. J.*, (1985), February, 89–100.
7. Constantinides, G.N. and A.C. Payatakes, "Network Simulation of Steady-State Two-Phase Flow in Consolidated Porous Media," *AIChE J.*, (1996) **42**, 2, 369–382.
8. Blunt, M. and P. King, "Macroscopic Parameters from Simulations of Pore Scale Flow," *Phys. Rev. A*, (1990) **42**, 8, 4780–4787.
9. Blunt, M.J., "Effects of Heterogeneity and Wetting on Relative Permeability Using Pore Level Modeling," *SPE J.*, (1997) **2**, March, 70–87.
10. Dias, M.M. and A.C. Payatakes, "Network Models for Two-Phase Flow in Porous Media Part 1. Immiscible Microdisplacement of Non-Wetting Fluids," *J. Fluid Mech.*, (1986) **164**, 305–336.
11. Mogensen, K. and E.H. Stenby, "A Dynamic Two-Phase Pore-Scale Model of Imbibition," *Transport in Porous Media*, (1998) **32**, 3, 299–327.
12. Dahle, H.K. and M.A. Celia, "A Dynamic Network Model for Two-Phase Immiscible Flow," *Computational Geosciences*, (1999) **3**, 1–22.
13. Bartley, J.T. and D.W. Ruth, "Relative Permeability Analysis of Tube Bundle Models," *Transport in Porous Media*, (1999) **36**, 2, 161–187.
14. Bartley, J.T. and D.W. Ruth, "Relative Permeability Analysis of Tube Bundle Models, Including Capillary Pressure," *Transport in Porous Media*, (2001) **45**, 3, 447–480.
15. Dong, M., F.A.L.Dullien and J.Zhou, "Characterization of Waterflood Saturation Profile Histories by 'Complete' Capillary Number," *Transport in Porous Media,* (1998) **31**, 2, 213-237.

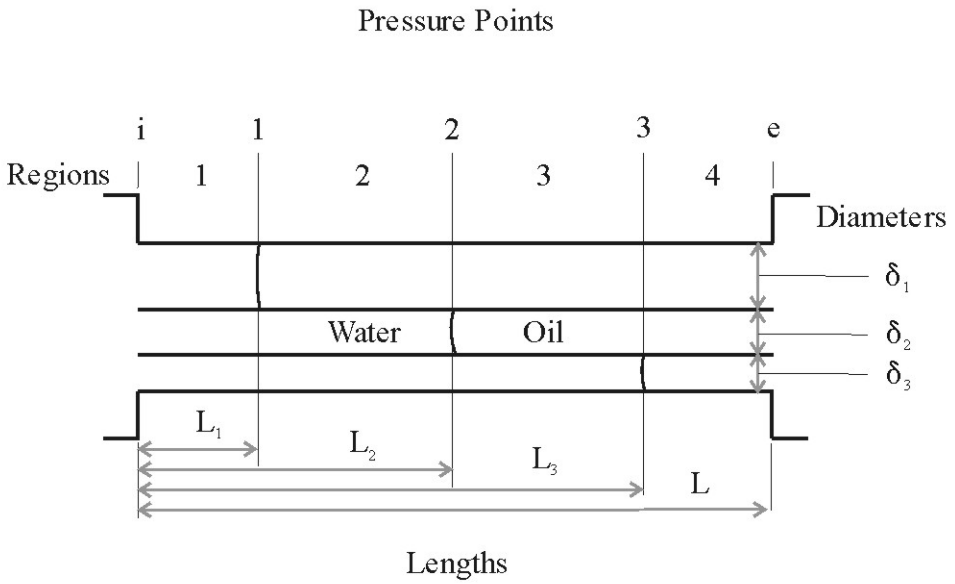

Fig 1 A schematic representation of the perfect-cross-flow model

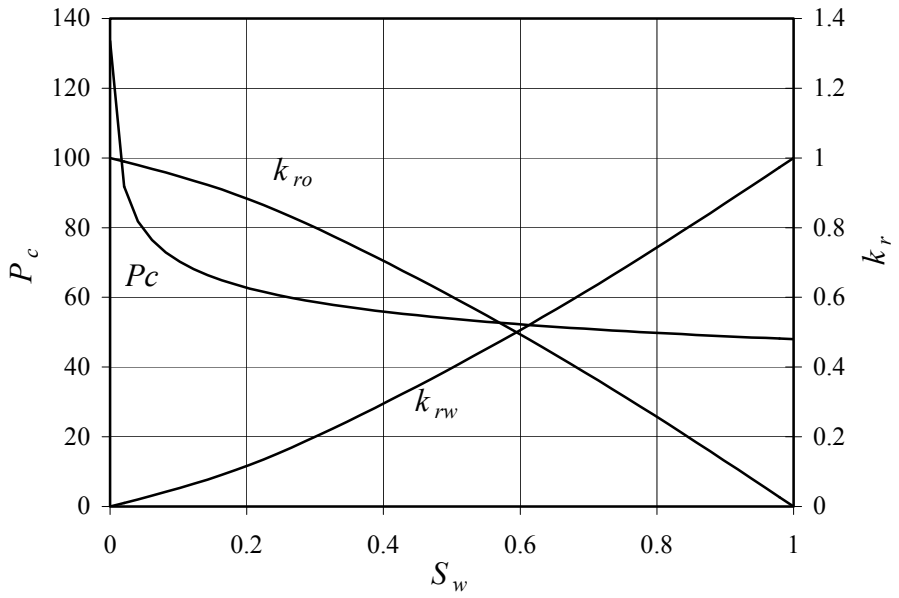

Fig 2. The capillary pressure and relative permeability curves for a λ=3 Corey medium.

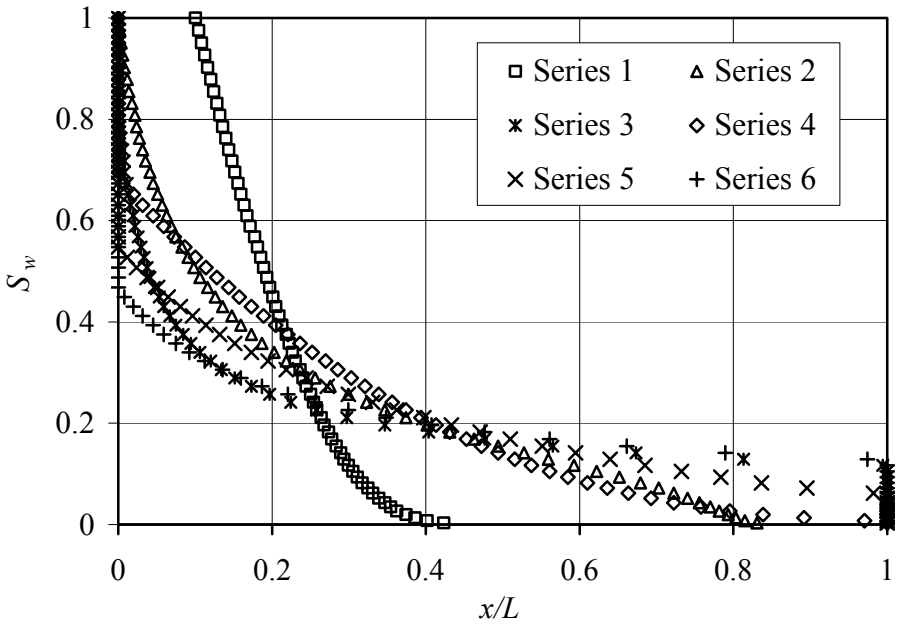

Fig 3 The saturation profiles at the time when 20% OOIP has been produced for various combinations of viscosity ratio and flow rate. The cases are Series 1: $Q_r=1,\mu_r=1$; Series 2: $Q_r=1,\mu_r=10$; Series 3: $Q_r=1,\mu_r=100$; Series 4: $Q_r=0.1,\mu_r=1$; Series 5: $Q_r=0.1,\mu_r=10$; Series 6: $Q_r=0.1,\mu_r=100$.

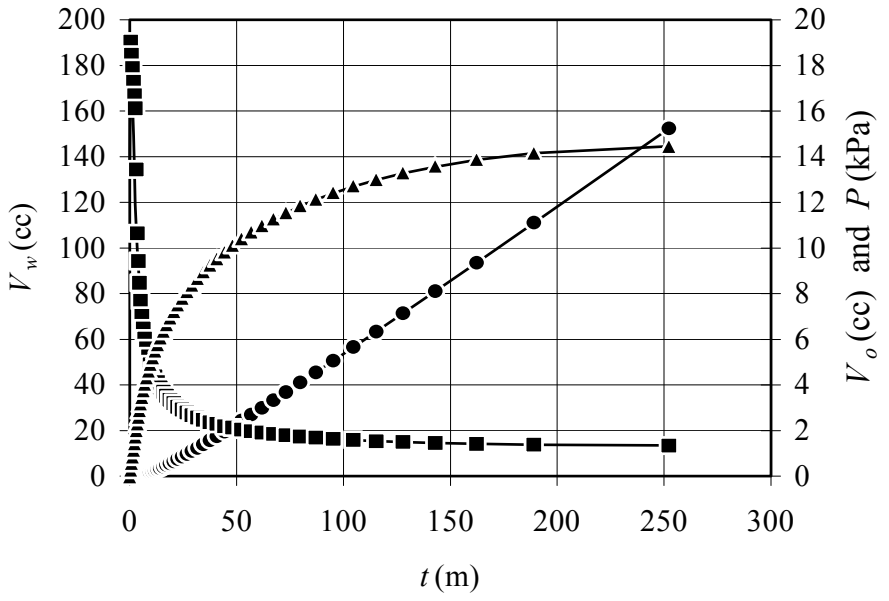

Fig 4. Comparison of MDL results (lines) with PCFM results for volumetric production of water (solid circles), volumetric production of oil (solid triangles), and pressure (solid squares) for a λ=3 Corey medium with $Q_r=0.1$ and $\mu_r=10$.

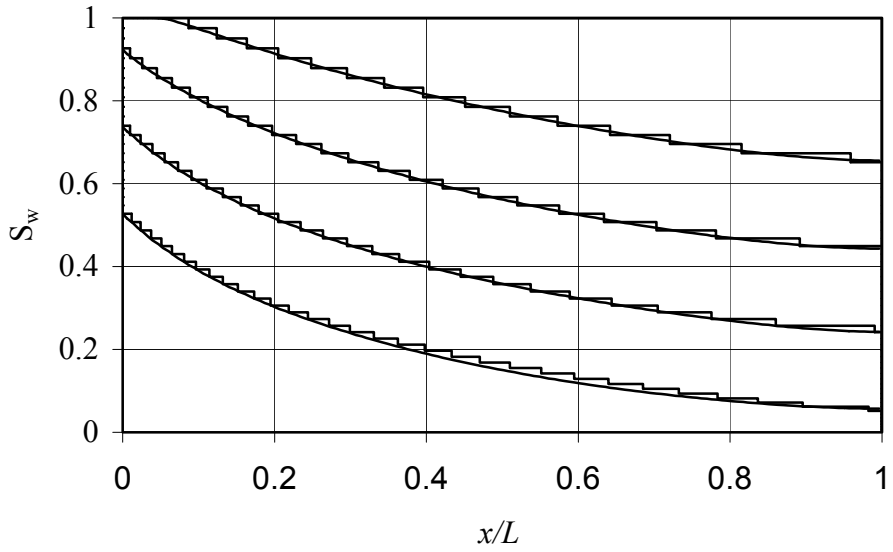

Fig 5. Comparison of MDL results with PCFM results for saturation profiles for a λ=3 Corey medium with $Q_r=0.1$ and $\mu_r=10$. The steps correspond to the PCFM and the lines are the MDL simulations.

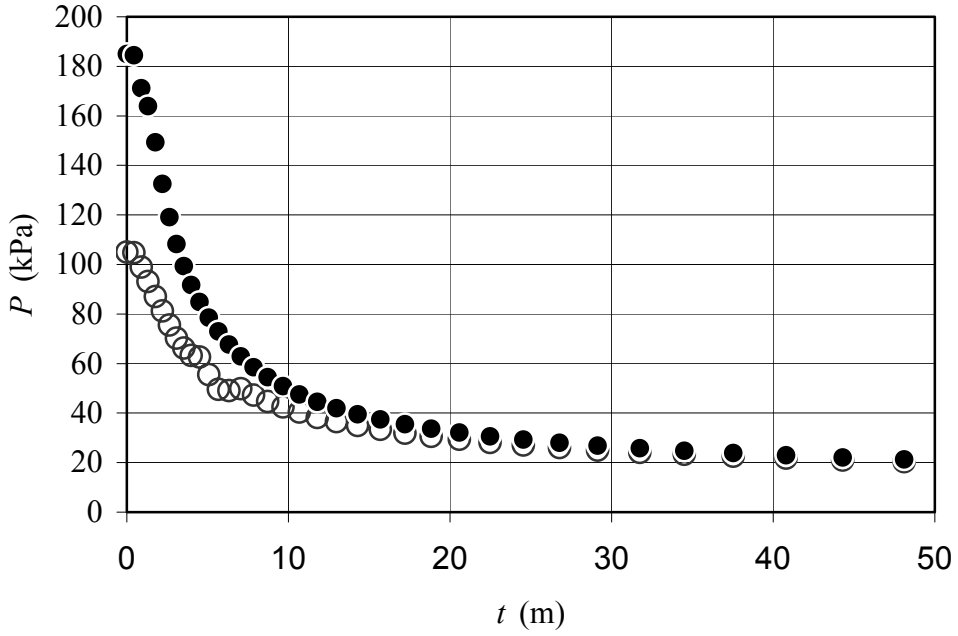

Fig 6. The differential pressure across the PCFM for a λ=3 Corey medium with $Q_r=0.1$ and $\mu_r=10$. The solid circles correspond to the saturation dependent boundary condition; the open circles correspond to the PCFM defined boundary condition.